Scanning laser imaging of dissipation in $YBa_2Cu_3O_{7-\delta}$-coated conductors

D. Abraimov,[a] D. M. Feldmann, A. A. Polyanskii, A. Gurevich, G. Daniels, and D. C. Larbalestier
University of Wisconsin, Applied Superconductivity Center, Madison, Wisconsin 53706

A. P. Zhuravel
Institute for Low Temperature Physics and Engineering, Kharkov, Ukraine

A. V. Ustinov
Physikalisches Institut III, Universität Erlangen-Nürnberg, Erlangen, Germany

(Received 6 May 2004; accepted 16 July 2004)

We investigate dc-current flow in high-j_c $YBa_2Cu_3O_{7-\delta}$-coated conductors by low-temperature laser scanning microscopy (LTLSM) and correlate the LTLSM response to magneto-optical imaging (MOI) and grain boundary (GB) misorientation. Because the voltage response measured by LTLSM is associated with the local electric field, while MOI shows the local magnetic field, the combination of these two techniques unambiguously shows that the dominant sources of dissipation and easy flux flow occur at and near GBs. By correlating LTLSM images to grain misorientation maps determined by electron backscatter diffraction (EBSD), we can directly observe the overloading of current paths through low-angle GBs neighboring higher-angle GBs. © *2004 American Institute of Physics*. [DOI: 10.1063/1.1794377]

Coated conductors (CC) using $YBa_2Cu_3O_{7-\delta}$ (YBCO) thin films with critical current densities (j_c) up to 3–4 MA/cm^2 at 77 K[1,2] are very promising materials for power applications of superconductors. However, MOI has shown that even such high-j_c conductors still have many current-limiting extended defects,[3] and their j_c values are seldom more than half the single crystal or intragrain values.[4] Spatially resolved MOI measurements have considerable utility in revealing very nonuniform current flow in CC and in helping raise j_c in CC. However, there have been no direct measurements of the electric field distribution $E(x,y)$, which is a very important characteristic of current-carrying capability of CC. The critical current I_c is usually defined at the mean electric field $E_c=1$ μV/cm, but local $E(x,y)$ can vary by several orders of magnitude due to current redistribution around macroscopic defects. Recent calculations of $E(x,y)$ around planar obstacles have shown that such hotspots of strong electric field near macroscopic defects can significantly limit global I_c (Ref. 5) and thermal stability[6] of CC. To truly understand what controls I_c, it is therefore important to correlate the local E distribution with structural inhomogeneities. In this letter we apply the LTLSM method[7,8] to a typical CC and estimate the E distribution using voltage response maps made on the YBCO. We correlate these LTLSM patterns measured in Erlangen with easy magnetic flux penetration patterns measured in Madison by MOI and grain misorientations obtained by EBSD.

We investigated YBCO CC of thickness 1 μm grown by *ex situ* conversion of BaF_2 based precursor[2] on [001]-textured Ni–W substrates. The average grain size of the substrate was about 40 μm. The GB distribution of the Ni–W substrate is replicated by YBCO. Bridges 50–250 μm wide and 0.1–1 mm long were laser patterned and contacts made with aluminum wire of 25 μm in diameter, using Ag-paste to gold contact pads deposited by shadow evaporation.

The LTLSM voltage response δV_ω map was measured at zero magnetic field and constant bias current I_b, using a low power scanning laser beam of diameter 1.6 μm. The beam intensity was modulated at the frequency $\omega/2\pi=102$ kHz at which δV_ω was measured. The spatial resolution was determined by the thermal length $l_\omega=(\kappa/C\omega)^{1/2}\simeq 3$–4 μm over which the temperature $T_\omega(x,y)$ decays along the film, where C is the heat capacity and κ is the thermal conductivity. In our experiment the dominant part of δV_ω was due to local heating by the beam. Since the YBCO film thickness $d\approx 1$ μm is smaller then l_ω, we treat $\delta V_\omega(x,y)$ as a 2D map. Comparison of δV_ω with the local reflectivity has shown that heat absorption was homogeneous over our samples. A representative $\delta V_\omega(x,y)$ map is shown in Fig. 1(b), where darker regions correspond to higher δV_ω response. This response is similar to that measured by low temperature scanning electron microscopy.[9]

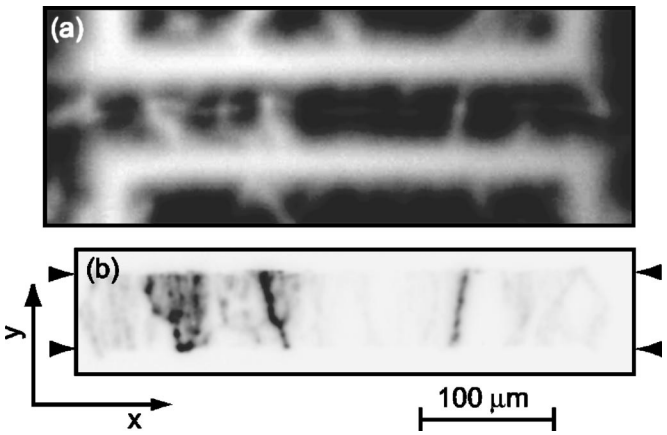

FIG. 1. (a) Zero field cooled magneto-optical image measured at $T=11.6$ K, $H=1000$ Oe. The narrow light horizontal line is due to domain structure in the imaging film. (b) δV response measured in low temperature scanning laser microscope at $T=78.9$ K and the bias current $I_b=287$ mA, the averaged electric field $\bar{E}=20.7$ mV/cm. The maximum response amplitude is 22 μV. Scanning step is 0.5 μm.

[a]Electronic mail: abraimov@cae.wisc.edu

We compare the δV_ω map with regions of easy flux penetration revealed by MOI shown in Fig. 1(a). The sample was zero field cooled (ZFC) to 11.6 K and then an external magnetic field of 1000 Oe above the field of full flux penetration was applied perpendicular to the film. Light areas in Fig. 1(a) correspond to regions of easy flux penetration while dark areas correspond to higher j_c regions. As was shown earlier by comparative MOI and EBSD,[10] magnetic flux penetrates into the YBCO along networks of GBs. Figure 1 shows a good correlation between the easy flux penetration channels and regions with high LTLSM response, δV_ω.

To link the LTLSM response $\delta V_\omega(x,y)$ to the local electric field $\mathbf{E}(x,y)$ caused by inhomogeneous current flow without the laser beam, we use the Maxwell equation:

$$\nabla \times \nabla \times \mathbf{E} = -\frac{4\pi}{c^2}\left(\sigma\frac{\partial \mathbf{E}}{\partial t} + \frac{\partial \mathbf{j}}{\partial T}\frac{\partial T}{\partial t}\right), \tag{1}$$

where $\mathbf{j}$ is the local current density and $\sigma(E,T)=\partial j/\partial E$ is the differential conductivity. Our LTLSM measurements were performed close to T_c where the mean electric field $\bar{E}$ ~ 20 mV/cm was much higher than $E_c=1$ μV/cm at which j_c is defined. In this case $\mathbf{j}\simeq\sigma\mathbf{E}$, where the ohmic flux flow conductivity σ is assumed to be uniform. The driving term $\propto\partial T/\partial t$ in Eq. (1) describes thermal perturbation of the electric field by a weak laser beam. In the linear response to the beam intensity, the solution of Eq. (1) is:

$$\delta E_{x\omega}(\mathbf{r},\mathbf{r}_0) = -\frac{1}{\sigma}\frac{\partial \sigma}{\partial T}\int G_\omega(\mathbf{r},\mathbf{r}')E_x(\mathbf{r}')T_\omega(\mathbf{r}',\mathbf{r}_0)d^2\mathbf{r}', \tag{2}$$

where $T_\omega(\mathbf{r}',\mathbf{r}_0)$ is the temperature response to the laser beam located at $\mathbf{r}_0(t)$. The Green's function $G_\omega(\mathbf{r},\mathbf{r}')$ varies on scales of the 2D skin depth, $\Lambda_{\text{eff}}=\Lambda^2/d$, where $\Lambda=(c^2/8\pi\sigma\omega)^{1/2}$ is the 3D skin depth. For the parameters of our LTLSM experiment, $\Lambda_{\text{eff}}\approx 253$ μm, so the temperature perturbation $T_\omega(\mathbf{r})$ varies on the thermal length l_ω much smaller than Λ_{eff}. Therefore, the main contribution to the integral in Eq. (2) comes from the small hot-spot area $|\mathbf{r}'-\mathbf{r}_0|<l_\omega$, so if $E_x(\mathbf{r})$ varies on scales much larger then l_ω, the local value $E_x(\mathbf{r})$ can be taken out of the integral. In this case Eq. (2) gives the LTLSM voltage response $\delta V_\omega=\int\mathbf{E}_\omega\mathbf{d}r$ in the form:

$$\delta V_\omega(\mathbf{r}_0) \approx -\frac{1}{\sigma}\frac{\partial \sigma}{\partial T}E_x(\mathbf{r}_0)\int \Gamma_\omega(\mathbf{r})d\mathbf{r}, \tag{3}$$

where the integration path connects the voltage leads and crosses $\mathbf{r}_0$, and the parameter $\Gamma_\omega(\mathbf{r})=\int G_\omega(\mathbf{r},\mathbf{r}')T_\omega(\mathbf{r}',\mathbf{r}_0)d^2\mathbf{r}'$ is proportional to the beam intensity and depends on cooling conditions. Thus, Eq. (3) predicts that the LTLSM voltage response $\delta V_\omega(\mathbf{r}_0)$ caused by the laser beam at point $\mathbf{r}_0$ is proportional to the local background electric field $E_x(\mathbf{r}_0)$ at the same point.

To verify Eq. (3) we measured δV_ω maps on a YBCO epitaxial films grown by pulsed laser deposition on $SrTiO_3$ single crystals.[11] The films were 250 nm thick, W=200 μm wide, and 2 mm long, a cut of 1 μm width and 0.1 W length was patterned perpendicular to the film edge. The steady-state distribution of $E(x,y)$ for this case was calculated by solving the nonlinear Maxwell equations by the hodograph method[5] for the power-law E-j characteristics, $E=(j/j_c)^nE_c$ with $n=6$. The results presented in (Fig. 2) indicate good qualitative agreement between measured $\delta V_\omega(x,y)$ and calculated $E_x(x,y)$. The strongest dissipation occurs at the tip of the defect, while $\delta V_\omega(x,y)$ is more extended in the direction perpendicular to the bias current.

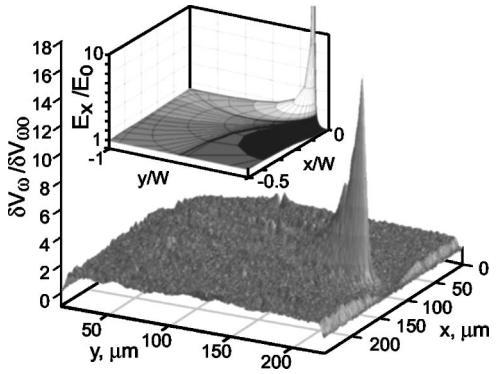

FIG. 2. δV_ω map in the vicinity of the defect described at 81 *K*, and $\bar{E}$ =28.2 mV/cm, where $\delta V_{\omega o}$ is the response measured far away from the defect. The inset shows $E_x(x,y)$ calculated by the hodograph method with $n=6$, where E_0 is the electric field at infinity (Ref. 5).

The above results indicate that the darker regions in Fig. 1(b) correspond to higher values of $E_x(\mathbf{r}_0)$. Since our CC samples were inhomogeneous on scales $\approx 10-40$ μm, much larger than the spatial resolution of the technique, we can spatially resolve regions of different vortex flow. The weakest channels in Fig. 1(b) are in the flux flow regime, while other regions with higher j_c may still be in the critical state.

Figure 3 shows more detailed information revealed by

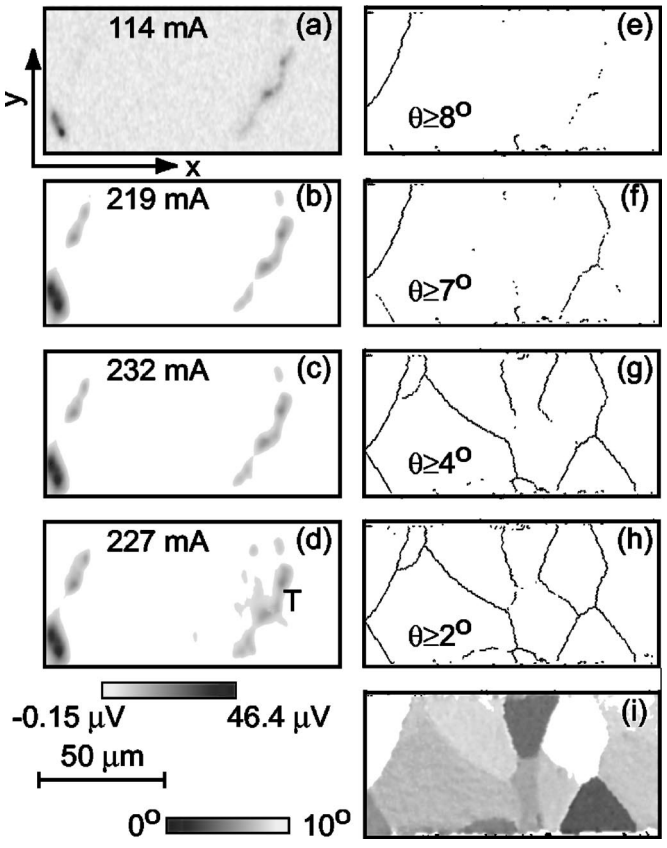

FIG. 3. (a)–(d) δV_ω responses measured at different bias currents at 81 K. The bias current is applied in the horizontal direction. Legend for δV_ω corresponds to the image (d); (e)–(h) GB misorientation maps; (i) *c*-axis misorientation map. Legend with angle limits corresponds to image (i).

LTLSM images taken at different bias currents. The figure compares the LTLSM response with the GB misorientation maps derived from EBSD measurements. Adequate Kikuchi patterns could not be obtained from the YBCO and thus the YBCO was etched off so as to reveal the YSZ buffer layer. Usually, the misorientation angles in the YBCO are $1°-2°$ lower than in the YSZ.[12,13]

In Fig. 3 a CC bridge section of 50 μm width by 112 μm length is imaged at I_b ranging from about I_c ($\approx$114 mA) to $2I_c$. At $I_b \approx I_c$ [Fig. 3(a)] it is clear that dissipation occurs preferentially in just two channels, one at the bridge left and one towards the right. Moreover, $E(x,y)$ is not uniform even within each channel. By comparison to the GB map in Fig. 3, it is clear that both channels lie along GBs and also [by comparing Fig. 3(a) to Figs. 3(e) and 3(f)] that the total YSZ grain-to-grain misorientation is $>8°$ for the major part of the left GB and about 7° for the right-hand GB. As I_b is raised towards twice I_c [Figs. 3(b)–3(d)], dissipation appears more broadly at lower and lower angle GBs and within the grain immediately to the left of the right-hand dissipative GB in Fig. 3(a). Such δV_ω patterns are consistent with vortices channeling along GBs.[11,14] It is striking that the major dissipation at 227 mA, approximately twice I_c, is still associated with the initially dissipative channels and is highly nonuniform. This has important implications for thermal stability of CC in applications.[6]

It is also noteworthy that the major LTLSM signal appears in the lower part of the left-hand GB. This left-hand GB is seen from the EBSD misorientation map to be composed of a major upper portion for which the YSZ misorientation is about 9° with a smaller lower portion whose misorientation is between 4° and 7°. The LTLSM shows that the lower angle segment has higher electric field because current flow is focused preferentially through the lower-angle, higher-j_c GB. This is analogous to the peak in the electric field observed at the end of the artificial defect in Fig. 2 and Ref. 5. The gradual onset of dissipation channels normal to current flow, for example in Figs. 3(c) and 3(d), is consistent with dissipative flux jets emanating from GB ends, such as the GB triple point seen at point *T* in Fig. 3(d).

One of the authors, D.A. thanks O. Turutanov and A. K. Feofanov for support with the data acquisition program. This work was supported by the AFOSR MURI Office and DOE-OETD.

[1] W. Zhang, X. Li, T. Kodenkandath, D. T. Verebelyi, U. Schoop, C. Thieme, M. W. Rupich, N. Nguyen, E. Siegal, and J. Lynch, Mater. Res. Soc. Symp. Proc. **EXS-3**, EE3.2.1 (2004).
[2] X. Li, M. W. Rupich, W. Zhang, N. Nguyen, T. Kodenkandath, U. Schoop, D. T. Verebelyi, C. Thieme, M. Jowett, P. N. Arendt, S. R. Foltyn, T. G. Holesinger, T. Aytug, D. K. Christen, and M. P. Paranthaman, Physica C **390**, 249 (2003).
[3] D. Larbalestier, A. Gurevich, D. M. Feldmann, and A. Polyanskii, Nature (London) **414**, 368 (2001).
[4] D. M. Feldmann, D. C. Larbalestier, D. T. Verebelyi, W. Zhang, Q. Li, G. N. Riley, R. Feenstra, A. Goyal, D. F. Lee, M. Paranthaman, D. M. Kroeger, and D. K. Christen, Appl. Phys. Lett. **79**, 3998 (2001).
[5] M. Friesen and A. Gurevich, Phys. Rev. B **63**, 064521 (2001).
[6] A. Gurevich, Appl. Phys. Lett. **78**, 1891 (2001).
[7] C. C. Chi, M. M. Loy, and D. C. Cronemeyer, Appl. Phys. Lett. **40**, 437 (1982); V. A. Konovodchenko, A. G. Sivakov, and A. P. Zhuravel, Cryogenics **26**, 531 (1986); K. A. Korolev, P. M. Shadrin, J. S. Preston, R. A. Hughes, J. K. Nam, and V. V. Pavlovskii, Physica C **341-348**, 1435 (2000); B. E. Klein, S. Seo, C. Kwon, B. H. Park, and Q. X. Jia, Rev. Sci. Instrum. **73**, 3692 (2002).
[8] A. G. Sivakov, A. V. Lukashenko, D. Abraimov, P. Müller, A. V. Ustinov, and M. Leghissa, Appl. Phys. Lett. **76**, 2597 (2000).
[9] R. Gross and D. Koelle, Rep. Prog. Phys. **57**, 651 (1994).
[10] D. M. Feldmann, J. L. Reeves, A. A. Polyanskii, G. Kozlowski, R. R. Biggers, R. M. Nekkanti, I. Maartense, M. Tomsic, P. Barnes, C. E. Oberly, T. L. Peterson, S. E. Babcock, and D. C. Larbalestier, Appl. Phys. Lett. **77**, 2906 (2000).
[11] A. Gurevich, M. S. Rzchowski, G. Daniels, S. Patnaik, B. M. Hinaus, F. Carillo, F. Tafuri, and D. C. Larbalestier, Phys. Rev. Lett. **88**, 097001 (2002).
[12] D. M. Feldmann, Ph.D. thesis, University of Wisconsin-Madison, 2001.
[13] L. Fernández, B. Holzapfel, F. Schindler, B. de Boer, A. Attenberger, J. Hänisch, and L. Schultz, Phys. Rev. B **67**, 052503 (2003).
[14] M. J. Hogg, F. Kahlmann, E. J. Tarte, Z. H. Barber, and J. E. Evetts, Appl. Phys. Lett. **78**, 1433 (2001).